University of Baghdad
College of Engineering
JOURNAL OF ENGINEERING

Journal of Engineering
journal homepage: www.jcoeng.edu.iq
Volume 31 Number 9 September 2025

Theoretical and Experimental Investigation of an Acetone-Filled Pulsating Heat Pipe Heat Exchanger for Waste Heat Recovery

Noor Ali Moayad *, Wail Sami Sarsam

Department of Mechanical Engineering, College of Engineering, University of Baghdad, Baghdad, Iraq

ABSTRACT

In this work, a vertical pulsating heat pipe heat exchanger (PHPHE) was designed for waste heat recovery, exchanging thermal energy between two air streams in a counterflow configuration. The heat exchanger consists of six rows, each row consists of one pulsating heat pipe (PHP), and each PHP has six turns. The working fluid used in the heat pipe was acetone with fill ratios of 50%, 60%, and 70%. The effect of evaporator inlet temperature at 40, 45, and 50°C and air velocity at 0.5, 0.7, and 0.9 m/s on the pulsating heat pipes consisting of three sections- evaporator, condenser, and adiabatic, whose dimensions were 25 x 25 x 10 cm, was studied. At the same time, the condenser temperature was maintained at 26°C. The system's thermal resistance, effectiveness, and heat transfer were calculated using Engineering Equation Solver (EES) software. Results showed that the device's efficiency ranged from approximately 15% to 32%. The device performed better at a 50% fill ratio compared to other ratios, achieving high efficiency at low speeds.

Keywords: Pulsating heat pipe, Waste heat recovery, Acetone, Heat exchanger.

1. INTRODUCTION

In the present day, the efficient recovery of waste heat during energy production and conversion has garnered significant attention. Accelerating global energy consumption has led to significant environmental and economic issues. Heat recovery stands out as a vital strategy for improving energy conversion efficiency and economic impacts **(Omar et al., 2019; Saghafifar et al., 2019)**. During industrial activities, heat is continuously produced and released into the environment as waste. Waste heat is typically divided into three categories: low-temperature (below 120°C), medium-temperature (120 °C to 650 °C), and high-temperature (above 650°C) **(Yang et al., 2020)**. The release of waste heat leads to energy waste and adds to heat pollution; thus, waste heat recovery is required to enhance energy conservation and lessen heat pollution. Traditionally. Over the last several decades, heat pipes have been extensively used as a typical essential passive device with high thermal conductivity, and heat pipes have been widely used for cooling electronic equipment such as

*Corresponding author
Peer review under the responsibility of University of Baghdad.
https://doi.org/10.31026/j.eng.2025.09.12

Article received: 17/04/2025
Article revised: 28/06/2025
Article accepted: 13/07/2025
Article published: 01/09/2025

laptop computers and smartphones and recovering waste heat through heat pipe heat exchangers **(Chaudhry et al., 2012; Yang et al., 2017).** Among numerous heat recovery systems, the heat pipe heat exchanger has recently gained popularity owing to its advantages, including a simple structure, no cross-contamination between fresh and exhaust air, high heat transfer efficacy, minimal pressure loss, and lower power consumption. Wickless heat pipe, Wick heat pipe, and thermosiphon(loop) heat pipe are the three most prevalent heat exchangers utilising heat pipes in HVAC systems **(Vakiloroaya et al., 2014)**. Note that pulsating heat pipe (PHP) is a prospective new member of the heat pipe family that is also gaining popularity for heat recovery applications **(Wang et al., 2016)**.

Unlike the standard heat pipe with a wick structure within **(Famouri et al., 2014),** PHP is always a closed-looped/open-looped serpentine-style wickless capillary tube that is evacuated and partially occupied by the working fluid. **(Akachi, 1993)** Launched the closed-loop pulsating heat pipe (CLPHP) globally in 1993. When the PHP is heated in one part (the evaporator) and cools down in another part (the condenser), the vapour-liquid plugs train's unique oscillatory mass and heat transfer, fueled by the saturation pressure difference between the evaporator and condenser, enables effective heat exchange between the two. Under unique conditions, the PHP, characterized by the interval unbalanced pressure oscillation and the sufficiently small scale of the meandering capillary, can, in specific circumstances, work successfully anti-gravity operation (for example, when heated from the top and cooled from the bottom)**(Riehl and dos Santos, 2012).** This distinctive capability garners significant attention towards its applications in heat recovery from the top to the bottom. Since the year 2000, numerous studies on PHPS have been conducted to determine the impact of different elements on the effective initiation of the pulsing movement of the working fluid and the PHPS thermal performance. **(Tseng et al., 2018)**. Transparent PHPS were also subjected to experiments to view the fluid flow and better explain their thermal performance **(Tseng et al., 2014; Youn and Kim, 2012).** According to published results, the working fluid's inner diameter and thermophysical characteristics must match the requirements for the capillary tube's working fluid when it is partly filled to separate into liquid slugs and vapour plugs sequentially after filling, enabling the pulsating movement to begin **(Chien et al., 2012)**.

According to the criterion, the bond number of the pulsating heat pipe, expressed as $D\sqrt{(g\Delta\rho/\sigma)}$, must be maintained within the range of 0.7 to 1.8. The PHP's inner diameter and the fluid's density differential between its liquid and vapour phases, surface tension, and gravity acceleration are represented by D, ρ, g, and σ, respectively. According to experimental results, a Bond number of 3.39 to 4 corresponds to the maximum diameter limit for an operable, terrestrial-based PHP **(Taft et al., 2012)**. With cautious Bond number of 3.39, the maximum diameter may be estimated using Eq. 1 put numbers for the equations

$$D_{max} = 1.84\sqrt{\frac{\sigma}{g(\rho_l-\rho_v)}} \quad (1)$$

Similarly, it has been discovered that a minimum diameter is required to sustain the slug plug flow necessary for a PHP to function properly. The minimal operating diameter is generally equivalent to a Bond number of 0.36 to 0.49 . Using a cautionary Bond number of 0.49, the minimum diameter may be computed using the equation.

$$D_{min} = 0.7\sqrt{\frac{\sigma}{g(\rho l-\rho v)}} \quad (2)$$

In this connection, several prior studies have been conducted to investigate the impacts of operating inclination on the thermal performance of the PHP. In fact, by adjusting the PHP's operation inclination angle, the impact of gravity on its operation may be characterized.

In general, while surface tension is considered higher than gravity within PHP, gravity is nevertheless shown to be important for PHP's thermal performance. The majority of published studies within the inclination angle range of 0-90° (from horizontal to vertical) denote that a PHP with a 90° inclination is vertically top-cooled and bottom-heated. Outperforms the other inclinations **(Liu et al., 2013)**. According to these investigations, without the help of gravity, the heat transmission capability of a PHP during horizontal operation is significantly reduced and even lost. However, additional studies show that a PHP may work well in a horizontal or anti-gravity posture **(Kearney et al., 2016)**. The meandering twists distinguish the capillary tube from other types of heat pipes. It is a component designed to be a U-shaped tube and linked to adjacent parallel tubes. The "meandering turn number" refers to the total number of meandering turns. The meandering bends are located in both the evaporator and the condenser sections. The number of meandering turns corresponds to the boiling points in the evaporator section. However, as the number of meandering turns increases, so does the CLPHP's heat transmission rate. However, a reasonable number of meandering turns may be predicted using the empirical correlation established in the previous work **(Kammuang-Lue et al., 2018)**. Alongside research examining how the number of meandering turns influences the thermal performance of the CLPHP, additional studies have investigated how various other factors impact thermal performance, leading to the following conclusion: Effects of evaporator section lengths**(Wang et al., 2015; Zhan et al., 2023)**, condenser length **(Kim and Kim, 2018)**, adiabatic section length **(Kammuang-lue et al., 2022)**, internal diameters **(Bhramara, 2018; Cheng and Wong, 2024)**, working fluids **(Borkar and Pachghare, 2015; Nekrashevych and Nikolayev, 2019)**, filling ratios **(Patel and Kumar, 2022; Rudresha et al., 2023)**, working orientations **(Nekrashevych and Nikolayev, 2019)**, and heat inputs **(Xu et al., 2022)**. In addition, experimental investigations of heat transfer mechanisms **(Jo et al., 2019)**. **(Shi et al., 2024)** The impact of evaporating-condensing length ratio and heat flux on the beginning and operating characteristics of a pulsating heat pipe was investigated. A crucial number is essential to ensure that the PHP works independently of gravity when determining the number of rotations. There are no definite standards in the literature for the optimal number of rotations. Increasing the number of turns improves PHP performance, as does increasing the evaporator heat supply area **(Bastakoti et al., 2018)**. Furthermore, the PHP performs better as channel density increases **(Winkler et al., 2020)**. An increasing number of PHP turns was found to improve device performance **(Karthikeyan et al., 2013)**, but it may simultaneously decrease the number of applications, as integrating them into a consolidated system becomes more difficult and can result in a loss of compression, as noted by **(Mameli et al., 2012)**. One of the researchers conducted an experimental study on a spring-loaded heat pipe heat exchanger to save energy in summer air conditioning systems. The working fluid used was R134a at a filling rate of 50% **(Yang et al., 2019)**.

This research will investigate the thermal efficiency of a pulsating heat pipe heat exchanger (PHPHE) that will be utilized for heat recovery from air to air, employing acetone as the working fluid. It will specifically analyze the impacts of varying filling ratios (50%, 60%, and 70%) and different air velocities (0.5, 0.7, and 0.9 m/s) on the system's thermal effectiveness and resistance. To accurately represent the realistic conditions faced by air conditioning systems in Iraq, hot air will be introduced to the evaporator at temperatures of 40, 45, and 50 degrees Celsius, reflecting typical and sometimes extreme summer temperatures across many Iraqi regions. The condenser will receive air at 26 degrees Celsius, the usual temperature at which air conditioning units are set in buildings. Selecting these values will

help to achieve initial cooling of the hot air before it enters the air conditioning system, thereby reducing the thermal load on the air conditioner and enhancing heat recovery efficiency. The PHP will be configured to function vertically, with bottom heating and a condenser cooled by a cooling coil system. The study intends to determine the best combination of operational parameters that will improve heat transfer efficiency, lower thermal resistance, and enhance overall energy recovery performance.

2. THERMAL ANALYSIS EQUATIONS

According to the experimental configuration, the following equations may be used to determine the heat energy transferred between the airflow and the pulsating heat pipe (PHP) in both hot and cold air ducts:

$$Q_C = \dot{m_c} \times C_{p,c} \left(T_{c,out} - T_{c,in}\right) (W) \quad (3)$$

$$Q_h = \dot{m_h} \times C_{p,h} \left(T_{h,in} - T_{e,out}\right) (\mathrm{W}) \quad (4)$$

Where
Q_C , Q_h Heat transfer to cold and hot air (W)
$\dot{m_c}$, $\dot{m_h}$ The cold and hot air mass flow rate (kg/s)
$C_{p,c}$, $C_{p,h}$ The specific heat of both cold and hot air will be measured at a constant pressure (J/kg.°C).
Assuming sealed, insulated duct walls, the values from Eq. 3 and Eq. 4 should match for energy equilibrium between hot and cold airflow. Mass flow rates $\dot{m_c}$ and $\dot{m_h}$ at the inlet and outlet must be equal to satisfy mass balancing. The precision of our calculations is shown by using the average of Q_c and Q_h to find the heat transfer rate between the airflow and the heat exchanger. In an ideal system, $Q_h$would equal Q_c; however, in reality, especially in pulsating heat pipes, achieving this balance is difficult due to heat losses and measurement errors. Even with fiberglass insulation, small discrepancies occurred, leading me to use the Qavg ratio for a more accurate thermal representation.

$$Q_{avg.} = \frac{(Q_h + Q_c)}{2} \ (\mathrm{W}) \quad (5)$$

After measuring $Q_{avg.}$ the dimensionless efficacy of the heat exchanger containing a PHP may be determined using the equation below:

$$\text{Effectiveness} = \frac{Q_{avg.}}{Q_{max}} \quad (6)$$

Where: Qmax is the highest potential heat transfer rate (W), which is calculated as the product of the temperature differential between hot and cold air and the air's minimum heat capacity rate, Cmin.

$$Q_{max} = C_{min} \times (T_{ein} - T_{cin}) (\mathrm{W}) \quad (7)$$

The Cmin equals either whatever is lower: the thermal capacity rate of cold air, or the thermal capacity rate of hot air, C_h.
Eqs. (6) and (7) represent Ch and Cc, respectively.

$$C_h = \dot{m_h} \times C_{p,h}\left(\frac{\text{J}}{\text{°C.s}}\right) \quad (8)$$

$$C_c = \dot{m_c} \times C_{p,c}\left(\frac{\text{J}}{\text{°C.s}}\right) \quad (9)$$

Additionally, the thermal resistance of the PHP, denoted as R, is defined in the following manner to compare its performance with published data in the literature:

$$\text{R} = \frac{\frac{1}{4}(T_{e1}+T_{e2}+T_{e3}+T_{e4})-\frac{1}{4}(T_{c1}+T_{c2}+T_{c3}+T_{c4})}{Q_{avg.}}(\text{C°/W}) \quad (10)$$

Where $T_{e1}, T_{e2}, T_{e3}$and, T_{e4} represent the evaporating and condensing regions' respective surface temperatures.

3. EXPERIMENTAL WORK

3.1. Description of Experimental Setup

This study identifies the optimum experimental setup designed to assess the thermal performance of the PHPHE in air-to-air applications. The experimental setup includes a heat exchanger and equipment, as shown in **Fig.1**.

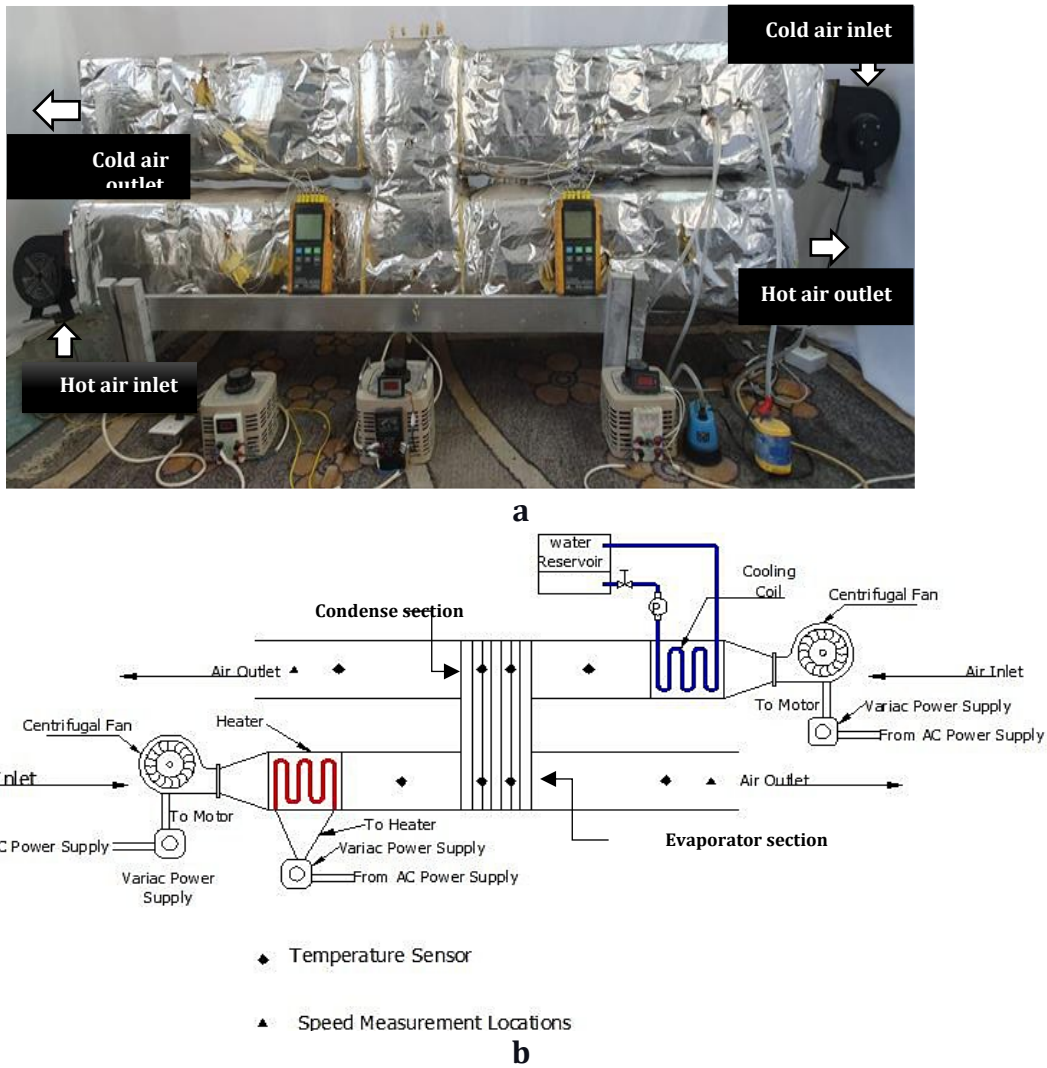

Figure1. a)The experimantal device , b) The schematic diagram device

It features two air channels linked to variable-speed centrifugal fans (FLJ Inflatable dedicated fan), regulated by variacs, alongside a 2500W finned heater, illustrated in **Fig. 2**. This heater serves as a hot air source, controlled by a 3 KVA Variac with the PHPHE. The experiment operates with reverse airflow, and the device is insulated with 4 cm of fiberglass to prevent heat loss. The closed-loop PHP consists of copper tubes, with evaporator, condenser, and adiabatic sections measuring 20 cm by 20 cm by 10 cm, respectively, and an inner diameter of 2.1 mm and outer diameter of 4 mm. The configuration includes six rows, each with one PHP containing six progressively arranged turns, as shown in **Fig. 3**. The adiabatic section is separated from the evaporator and condenser by two insulated plates. Iron skewers enhance the surface area along the evaporator and condenser. The PHPHE specifications are in Table 1, and they contain acetone at concentrations of 50%, 60%, and 70%. Fluid characteristics are in Table 2. The PHP features two valves for fluid charging and discharging and utilizes a type K thermocouple (±1%). Five thermocouples are placed at the evaporator inlet and outlet and at the condenser outlet, as shown in **Fig. 1b**.

The average temperature was recorded using one thermocouple at the condenser inlet and eight in the pulsed heat pipes. Four thermocouples were in the second and four in the fourth pulsed heat pipe, with two in the condenser and two in the evaporator regions of each pipe.

Figure 2. finned heater with a capacity of (2500W)

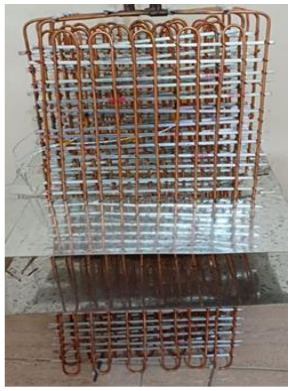

Figure 3. PHP arrangement

Table 1. Specifications of the PHPHE

Length x width x height (cm)	Condenser section length(cm)	Evaporator section length(cm)	Adiabatic section length(cm)	Inside diameter (mm)	Outside diameter (mm)	No. of terms	No. of rows
30x20x60	20	20	10	2.1	4	6	6

Table 2. Physical Properties of Acetone by using the EES program

T (°C)	P_{sat} (KPa)	$\rho_l(\frac{kg}{m^3})$	$\rho_v(\frac{kg}{m^3})$	$C_{p.l}$ $(\frac{kj}{kg.k})$	$C_{p,v}$ $(\frac{kj}{kg.k})$	$\mu_l\left(\frac{kg}{m\cdot s}\right)$ $x10^{-6}$	$\mu_v\left(\frac{kg}{m\cdot s}\right)$ $x10^{-9}$	Δh (kj/kg)	$\sigma\left(\frac{N}{m}\right)$ $x10^{-4}$
30	38.06	779	0.9031	2.156	1.419	294.6	7633	529.1	2208
40	56.53	767.7	1.309	2.182	1.473	270.7	7901	518.7	2084
50	81.61	756.1	1.848	2.211	1.53	249.8	8171	508.1	196
60	114.9	744.3	2.552	2.242	1.59	231.2	8444	497.2	1838
70	158.2	732.2	3.455	2.275	1.653	214.4	8719	485.8	1716

Table 3. Design parameters of the PHP.

Design parameter	Numerical value
Internal diameter	2.1mm
External diameter	4mm
Number of turns	6
Length	780 mm

3.2 Experimental Procedure

1-Before Charging the working fluid, the PHP was evacuated by using a vacuum pump linked to the filling valve until the internal pressure was reduced to -30psi. Upon reaching this pressure, the valves are sealed, and the requisite proportion of the necessary liquid is dispensed.

2-The evaporator temperature is controlled using a heater coupled to a 3-kVA AC variable voltage transformer (VARIAC). This research considers three evaporator temperatures: 40, 45, and 50 degrees.

3-The condenser temperature is regulated at 26 degrees using a cooling system that includes a cooling coil with a diameter of 1/4 inch connected to a water pump placed in a water basin.

4-A 1-kVA AC VARIAC controlled the speed of each centrifugal fan, allowing the air velocity in the evaporator and condenser ducts to be adjusted to 0.5, 0.7, and 0.9 m/s. The air velocity was equal in both ducts during all test runs.

5-The temperature-measuring device monitors the temperatures entering the condenser and evaporator. After the PHP system has stabilized, readings are obtained and used for the required computations. The procedure is reiterated at various temperatures and velocities.

6- The tubes are evacuated by an evacuator to remove the liquid and eliminate contaminants.

The same procedure is repeated for all cases. The PHPHE was initially subjected to a leak test to confirm its proper functioning before connection, ensuring the absence of leaks. This is accomplished by applying the bubble method, a solution of detergent and water to all coils and rows of the tubes, followed by directing high-pressure dry air using a compressor into each tube.

4. RESULTS AND DISCUSSION

A study was conducted to investigate the factors affecting the performance of an acetone-charged heat exchanger. Various parameters were examined, including the hot air input temperature (40, 45, and 50°C), the filling ratio (50, 60, and 70%), and the air velocity (0.5, 0.7, and 0.9 m/s). The air velocity in the evaporator and condenser zones remained equal. Qavg was calculated using Eq. 3, which relies on Qe and Qc as they are almost identical. The difference between them is due to heat losses across the walls of the air ducts. Since the system is not ideal, there is always heat loss across the walls. Heat loss depends on the airflow velocity and the evaporator temperature. As shown in **Fig. 4**, the heat transfer rate increases linearly with increasing evaporator temperature. Higher temperatures enhance heat transfer in the heat system between the inlet air temperature and the pulsating heat pipes' heat exchangers at the evaporator and condenser sections, according to Eq.3 and Eq.4. From the **Fig. 4**, It can be noted that at a low velocity (0.5 m/s), a decrease in air speed

reduces the heat transfer coefficient and the rate of heat transmission between the heat exchanger surface and the air, the temperature difference between the inlets and outlets of the evaporator and condenser is reduced.

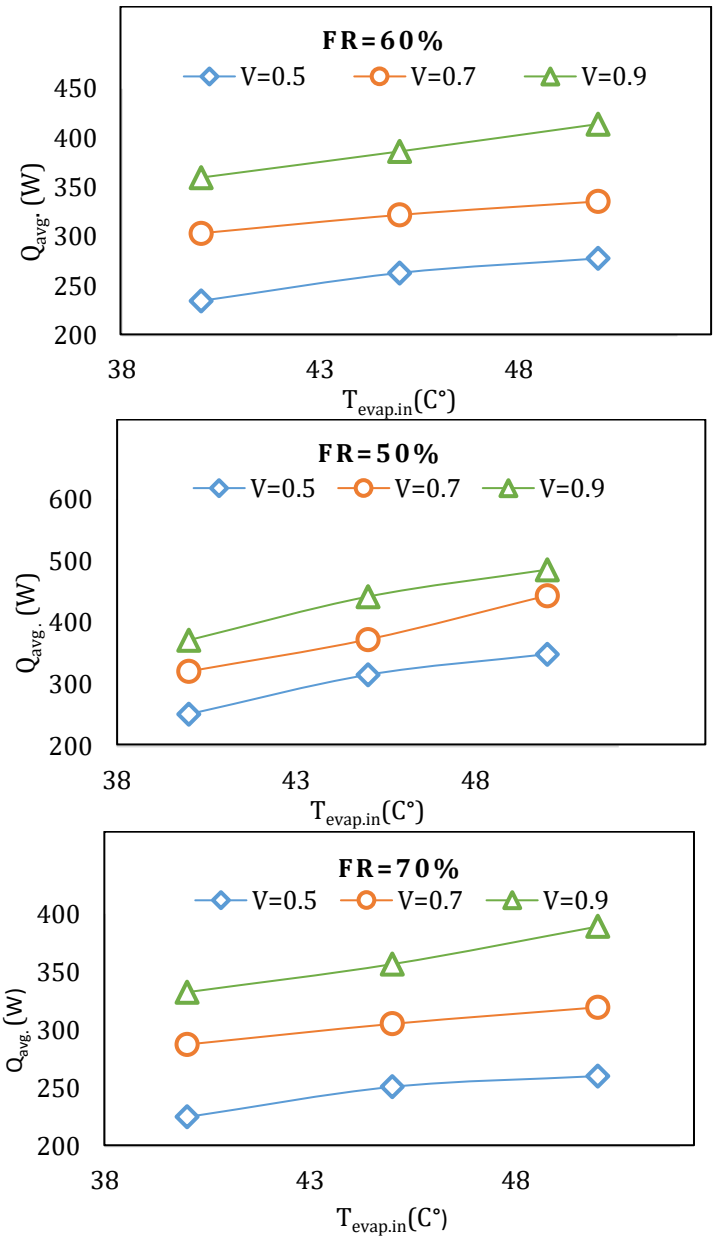

Figure 4. Average of transfer of heat rate to a heat exchanger's condenser and evaporator containing a PHP charged with acetone versus the hot air inlet temperature with FR = 50%, 60 %, and 70%

Fig. 5 The temperature differential between the evaporator and condenser air decreases with increasing air flow velocity, reducing the effective mass flow rate and resulting in a lower heat exchanger efficiency and a lower difference between the inlet air temperature and the heat pipe temperature. Therefore, efficiency is optimal at a flow velocity of 0.5, where the fluid is exposed to heat for a more extended period, resulting in increased heat dissipation. This enhances system efficiency and facilitates better heat transfer. This is

because the amount of heat transferred, Qactual, rises with higher speed, while the maximum heat, Qmax, rises faster, resulting in decreased efficiency at elevated speeds. Efficiency depends on the efficiency of heat absorption and dissipation. As the evaporator temperature increases, the system's ability to maintain thermal equilibrium decreases, leading to accelerated evaporation, which reduces the complexity of the heat exchange process. This can be understood through the rise in heat transfer; however, the actual increase in heat transfer is minimal when juxtaposed with the maximum possible temperature, since Qmax is significantly larger than Q_{actual}.

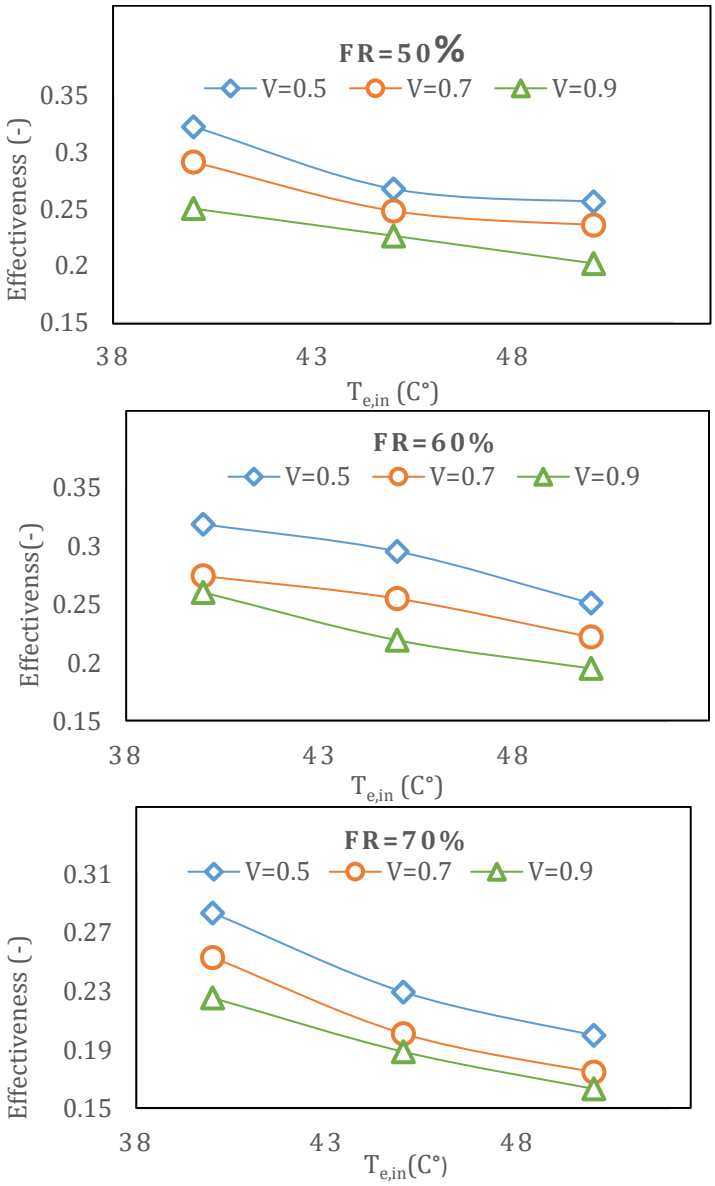

Figure 5. Effectiveness of a heat exchanger containing a PHP charged with acetone versus the hot air

We note that in **Fig. 6**, at a 50% fill ratio, efficiency is higher than at other ratios and the device's efficiency ranges from approximately 15% to 32. At 70%, efficiency decreases due to liquid pooling and the poor capillary properties of the tubes. Increasing the liquid fill ratio resulted in a decrease in efficiency. This is due to the increased thermal resistance between the evaporator and condenser sections as the liquid depth increases. The decrease in

efficiency with increasing temperature may be due to the use of two different materials: copper for the heat pipes and iron sheets placed along the evaporator and condenser to increase the surface area, as the two materials differ. It may also be due to the evaporator being the same length as the condenser. It lacks sufficient heat transfer area to achieve a higher heat transfer rate, resulting in increased thermal resistance and, at the same time, increased heat transfer, consequently decreasing effectiveness.

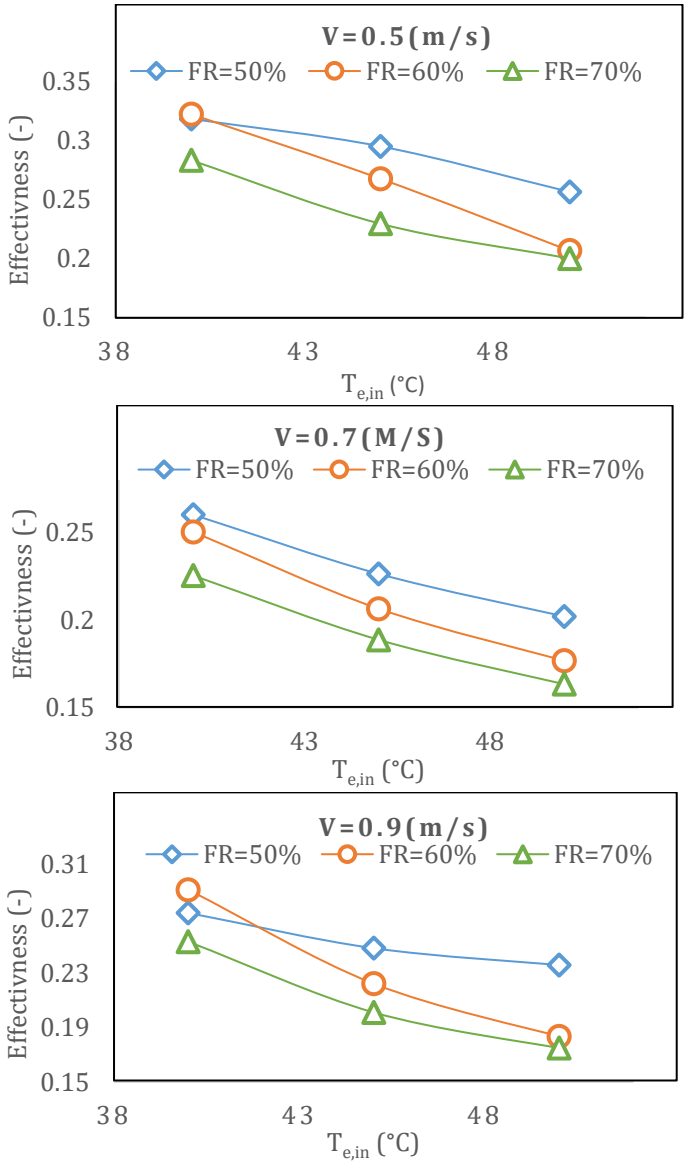

Figure 6. Effectiveness of a heat exchanger containing a PHP charged with acetone versus the hot air

Fig. 7 Shows that as the inlet temperature of the evaporator increases, thermal resistance increases because of the increase in the Temperature gradient and overall temperature ($T_{ein} - T_{cin}$) with increased heat transfer, but this increase in the temperature gradient is less than the overall temperature. When the velocity increases to 0.9, according to the thermal resistance relation in equation 9, there was an improvement in thermal resistance. This is due to increased convection heat transfer, resulting in a higher overall heat transfer

rate. Meanwhile, the temperature difference between the evaporator and condenser surfaces stayed nearly the same or increased slightly.

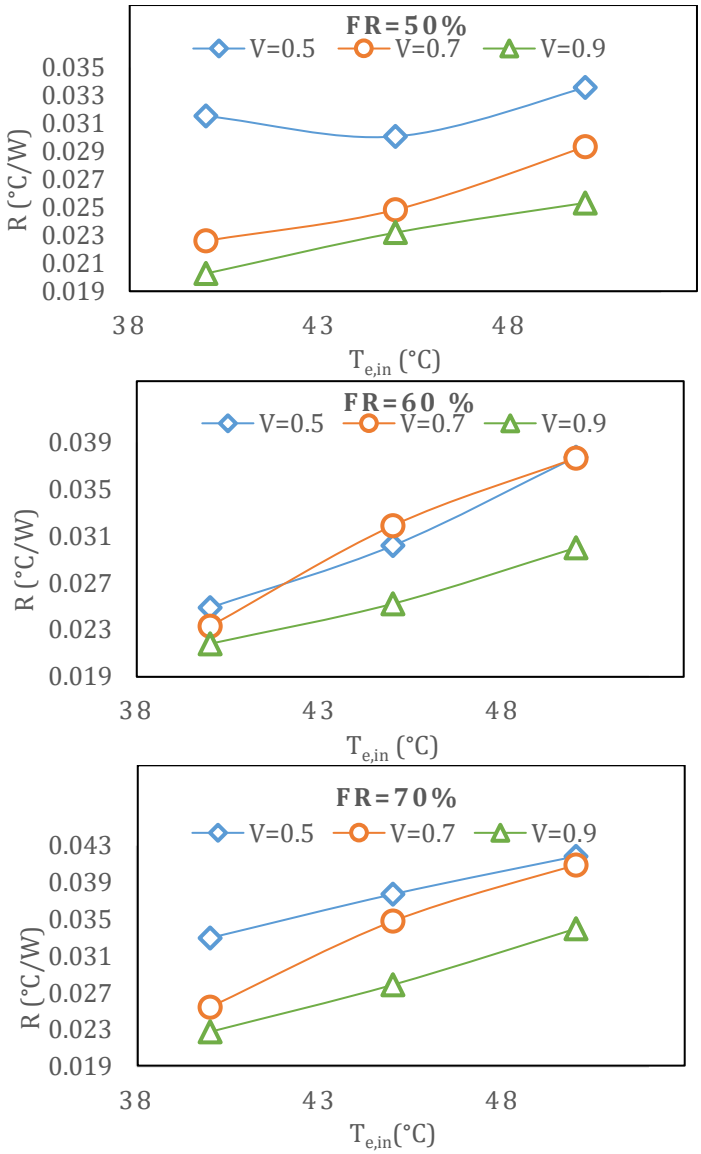

Figure 7. Thermal resistance of a heat exchanger containing a PHP charged with acetone versus the hot air inlet temperature with FR = 50%, 60% and 70%

Fig. 6 and **Fig. 8.** Heat resistance is larger at FR = 70% than at FR = 50% and 60%. This suggests that a high filling ratio may decrease heat transfer efficiency due to a reduction in the effective area for heat exchange and better fluid collection inside the tubes, resulting in increased resistance. At FR = 50%, thermal resistance is reduced, implying that this ratio may provide the optimal balance of fluid availability and effective heat transmission. We see that heat resistance increases with increasing filling ratio, with resistance being lower at FR = 50% and more excellent at FR = 70%. This suggests that a high filling ratio reduces the effective evaporation rate, increasing resistance. At high FR = 70%. Increasing fluid volume decreases the effective surface for heat transmission, slowing evaporation and improving thermal resistance. Fluid collection may form inside the tubes, impeding effective heat transfer.

To compare these findings with earlier research, **(Babu et al., 2018)** studied fill ratios ranging from 50% to 90% using acetone and discovered that the best thermal performance occurred at a 60% fill ratio, where they recorded the lowest thermal resistance. The differences between the outcomes of these studies and the current research can be attributed to variations in operating conditions and design aspects, namely:

- The installation angle set at 90° vertical in this study.
- The application of three distinct air velocities (0.5, 0.7, and 0.9 m/s).
- A different cooling mechanism for the condenser.
- Multiple Pulsed Heat Pipes were utilized.

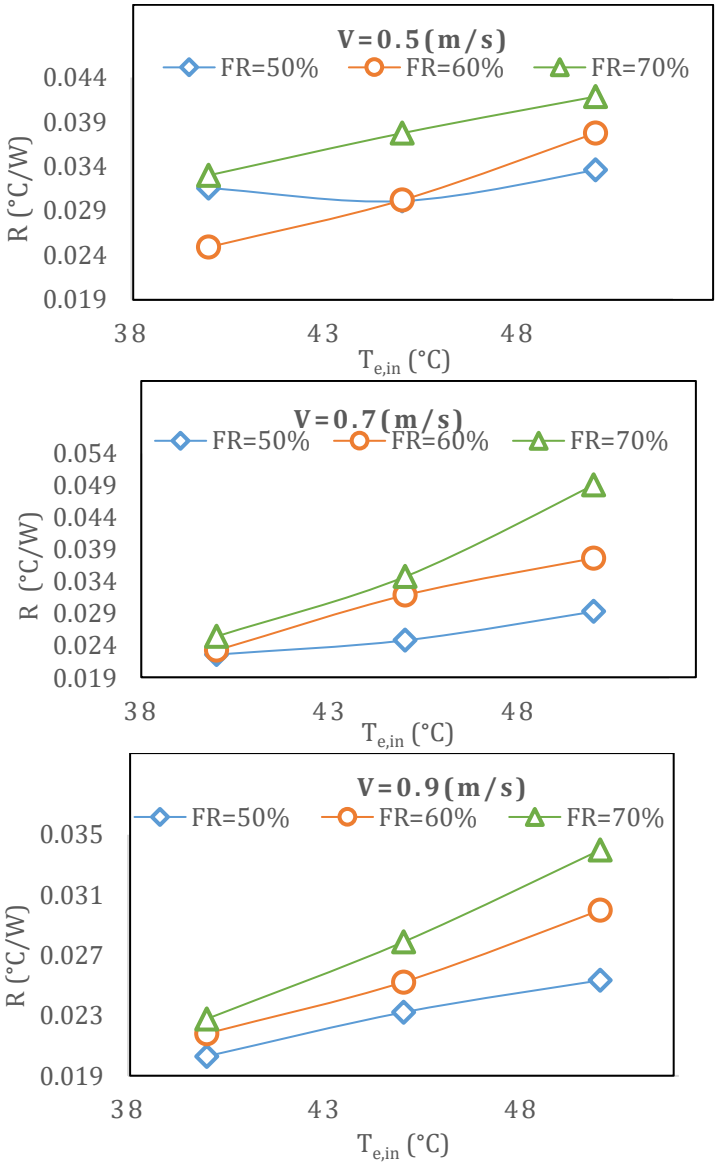

Figure 8. Effect of the fill ratio on the thermal resistance.

A study by **(Babu and Reddy, 2016)** revealed that acetone, methanol, and ethanol at filling ratios of 10% to 70% outperformed acetone at a 50% filling ratio, which is consistent with the current research findings. In this context, three air velocities were tested: 0.5, 0.7, and 0.9 m/s, with the study indicating that the highest thermal efficiency was reached at 0.5 m/s.

These findings regarding the effect of air velocity correlate with **(Yang et al., 2020)**, which indicated that 0.5 m/s yielded the highest efficiency.
In summary, the current study determined that the optimal conditions for thermal performance using acetone as the working fluid involved a 50% fill ratio. Conversely, 0.5 m/s was identified as most favorable for achieving peak thermal efficiency.

5. CONCLUSIONS

This study involved fabricating and testing heat exchangers utilizing pulsating heat pipes filled with acetone at 50%, 60%, and 70% ratios. The focus was on assessing both the effectiveness of the heat exchangers and the thermal resistance of the PHP, particularly at evaporator temperatures 40, 45, and 50 °C and airflow velocities 0.5, 0.7 and 0.9 m/s. Cold and hot air streams pass through the heat exchanger in a counter-flow configuration.
The findings indicate that:

1. The optimum filling ratio depends on the balance of fluid volume and heat exchange area. Results show that FR = 50% provides the lowest thermal resistance and best thermal efficiency, and the device's efficiency ranges from approximately 15% to 32%.
2. The thermal resistance increased with the increase in the inlet air temperature and was highest at low velocities and high filling ratios. On the contrary, at a 50% filling ratio and a velocity of 0.9 m/s, the lowest thermal resistance was observed, indicating improved heat transfer under these conditions. Effectiveness was found to decrease with increasing air velocity, with low velocities, such as 0.5 m/s, showing the highest heat transfer efficiency. So 0.5 is better because it provides better effectiveness.
3. Increasing the inlet temperature of the evaporator increases the heat transfer and reduces the efficiency. This is because the actual heat transfer increases slightly compared to the maximum heat transfer. The resistance increases due to the increase in the temperature gradient and the total temperature (T_ein - T_cin) with the increase in heat transfer, but this increase in the temperature gradient is less than the total temperature.

NOMENCLATURE

Symbol	Description	Symbol	Description
Q	Heat transfer (W)	R	Thermal resistance(C°/W)
$T_{e,in}$	Inlet evaporator temperature, °C	$T_{c,in}$	Inlet condenser temperature, °C
$T_{e,out}$	outlet evaporator temperature, °C	$T_{c,out}$	outlet condenser temperature, °C
m·	Mass flow rate	P_{sat}	Saturation pressure
ρ_l	Liquid density ($\frac{kg}{m^3}$)	ρ_v	Vipour density ($\frac{kg}{m^3}$)
μ_l	Dynamics viscosity of liquid	$C_{p,l}$	Specific heat capacity of liquid($\frac{kj}{kg.k}$)
μ_v	Dynamics viscosity of liquid	$C_{p,v}$	Specific heat capacity of liquid($\frac{kj}{kg.k}$)
hΔ	Latent heat(kj/kg)	σ	Surface tenseion(N/m)
Avg.	average	Min.	minimum

Acknowledgements

The author expresses gratitude to the entire team of the Mechanical Engineering Department at the College of Engineering, University of Baghdad, for their valuable help and guidance.

Credit Authorship Contribution Statement

Noor Ali Moayad : Writing – original draft, Writing – review & editing, Validation, Software, Methodology. Wail Sami Sarsam : Supervising and following up the research, Writing – review & editing,.

Declaration of Competing Interest

The authors declare that they have no known competing financial interests or personal relationships that could have appeared to influence the work reported in this paper.

REFERENCES

Akachi, H. 1993. Structure of micro-heat pipe. Washington, DC: U.S.

Babu, E., Reddappa, H., Reddy, G.G., 2018. Effect of filling ratio on thermal performance of closed loop pulsating heat pipe. *Materials Today: Proceedings*, 5(10), pp. 22229-22236. https://doi.org/10.1016/j.matpr.2018.06.588.

Bastakoti, D., Zhang, H., Li, D., Cai, W., Li, F., 2018. An overview on the developing trend of pulsating heat pipe and its performance. *Applied Thermal Engineering*, 141, pp. 305-332. http://dx.doi.org/10.1016/j.applthermaleng.2018.05.121.

Bhramara, P., 2018. CFD analysis of copper closed loop pulsating heat pipe. *Materials Today: Proceedings*, 5(2), pp. 5487-5495. https://doi.org/10.1016/j.matpr.2017.12.138.

Borkar, R., Pachghare, P., 2015. Effect of working fluid, filling ratio and number of turns on pulsating heat pipe thermal performance. *Frontiers in Heat Pipes (FHP)*, 6(1). http://dx.doi.org/10.5098/fhp.6.4.

Chaudhry, H.N., Hughes, B.R., Ghani, S.A., 2012. A review of heat pipe systems for heat recovery and renewable energy applications. *Renewable and Sustainable Energy Reviews*, 16(4), pp. 2249-2259. https://doi.org/10.1016/j.rser.2012.01.038.

Cheng, P.-S., Wong, S.-C., 2024. Detailed visualization experiments on the start-up process and stable operation of pulsating heat pipes: Effects of internal diameter. *International Journal of Heat and Fluid Flow*, 106, P. 109325. https://doi.org/10.1016/j.ijheatfluidflow.2024.109325.

Chien, K.-H., Lin, Y.-T., Chen, Y.-R., Yang, K.-S., Wang, C.-C., 2012. A novel design of pulsating heat pipe with fewer turns applicable to all orientations. *International Journal of Heat and Mass Transfer*, 55(21-22), pp. 5722-5728. http://dx.doi.org/10.1016/j.ijheatmasstransfer.2012.05.068.

Babu, E.R. and Reddy, G.G., 2016. Effect of working fluid and filling ratio on performance of a closed loop pulsating heat pipe. *Journal of Engineering Science and Technology*, *11*(6), pp. 872-880.

Famouri, M., Carbajal, G., Li, C., 2014. Transient analysis of heat transfer and fluid flow in a polymer-based micro flat heat pipe with hybrid wicks. *International Journal of Heat and Mass Transfer*, 70, pp. 545-555. https://doi.org/10.1016/j.ijheatmasstransfer.2013.11.019.

Jo, J., Kim, J., Kim, S.J., 2019. Experimental investigations of heat transfer mechanisms of a pulsating heat pipe. *Energy conversion and management*, 181, pp. 331-341. http://dx.doi.org/10.1016/j.enconman.2018.12.027.

Kammuang-Lue, N., Sakulchangsatjatai, P., Sriwiset, C., Terdtoon, P., 2018. Investigation and predictation of optimum meandering turn number of vertical and horizontal closed-loop pulsating heat pipes. *Thermal Science*, 22(1 Part A), pp. 273-284. https://doi.org/10.2298/TSCI150707161K.

Kammuang-lue, N., Sakulchangsatjatai, P., Terdtoon, P., 2022. Thermal performance of various adiabatic section lengths of closed-loop pulsating heat pipe designed for energy recovery applications. *Energy Reports*, 8, pp. 731-737. https://doi.org/10.1016/j.egyr.2022.10.149.

Karthikeyan, V., Ramachandran, K., Pillai, B., Solomon, A.B., 2013. Effect of number of turns on the temperature pulsations and corresponding thermal performance of pulsating heat pipe. *Journal of Enhanced Heat Transfer*, 20(5). https://doi.org/10.1615/JEnhHeatTransf.2014010509.

Kearney, D.J., Suleman, O., Griffin, J., Mavrakis, G., 2016. Thermal performance of a PCB embedded pulsating heat pipe for power electronics applications. *Applied Thermal Engineering*, 98, pp. 798-809. http://dx.doi.org/10.1016/j.applthermaleng.2015.11.123

Kim, J., Kim, S.J., 2018. Experimental investigation on the effect of the condenser length on the thermal performance of a micro pulsating heat pipe. *Applied Thermal Engineering*, 130, pp. 439-448. https://doi.org/10.1016/j.applthermaleng.2017.11.009.

Liu, X., Chen, Y., Shi, M., 2013. Dynamic performance analysis on start-up of closed-loop pulsating heat pipes (CLPHPs). *International Journal of Thermal Sciences*, 65, pp. 224-233. https://doi.org/10.1016/j.ijthermalsci.2012.10.012.

Mameli, M., Marengo, M., Zinna, S., 2012. Numerical model of a multi-turn closed loop pulsating heat pipe: effects of the local pressure losses due to meanderings. *International Journal of Heat and Mass Transfer*, 55(4), pp. 1036-1047. https://doi.org/10.1016/j.ijheatmasstransfer.2011.10.006.

Nekrashevych, I., Nikolayev, V.S., 2019. Pulsating heat pipe simulations: impact of PHP orientation. *Microgravity Science and Technology*, 31(3), pp. 241-248. https://doi.org/10.1007/s12217-019-9684-3.

Omar, A., Saghafifar, M., Mohammadi, K., Alashkar, A., Gadalla, M., 2019. A review of unconventional bottoming cycles for waste heat recovery: Part II–Applications. *Energy conversion and management*, 180, pp. 559-583. https://doi.org/10.1016/j.enconman.2018.10.088.

Patel, E.D., Kumar, S., 2022. The impact of variation in filling ratios, evacuation pressure, and heat input on thermal performance of pulsating heat pipe. *IEEE Transactions on Components, Packaging and Manufacturing Technology*, 12, pp. 259-269. https://doi.org/10.1109/TCPMT.2021.3139727.

Riehl, R.R., dos Santos, N., 2012. Water-copper nanofluid application in an open loop pulsating heat pipe. *Applied Thermal Engineering*, 42, pp. 6-10. https://doi.org/10.1016/j.applthermaleng.2011.01.017.

Rudresha, S., Babu, E., Thejaraju, R., 2023. Experimental investigation and influence of filling ratio on heat transfer performance of a pulsating heat pipe. *Thermal Science and Engineering Progress*, 38, P. 101649. https://doi.org/10.1016/j.tsep.2023.101649.

Saghafifar, M., Omar, A., Mohammadi, K., Alashkar, A., Gadalla, M., 2019. A review of unconventional bottoming cycles for waste heat recovery: Part I–Analysis, design, and optimization. *Energy conversion and management*, 198, P. 110905. https://doi.org/10.1016/j.enconman.2018.10.047.

Shi, W., Li, M., Chen, H., Pan, L., 2024. Effect of evaporating-condensing length ratio and heat flux on starting and operating characteristic of pulsating heat pipe. *Applied Thermal Engineering*, 246, P. 122963. https://doi.org/10.1016/j.applthermaleng.2024.122963.

Taft, B.S., Williams, A.D., Drolen, B.L., 2012. Review of pulsating heat pipe working fluid selection. *Journal of Thermophysics and Heat Transfer*, 26(4), pp. 651-656. https://doi.org/10.2514/1.T3768.

Tseng, C.-Y., Wu, H.-M., Wong, S.-C., Yang, K.-S., Wang, C.-C., 2018. A novel thermal module with 3-D configuration pulsating heat pipe for high-flux applications. *Energies*, 11(12), P. 3425. http://dx.doi.org/10.3390/en11123425.

Tseng, C.-Y., Yang, K.-S., Chien, K.-H., Jeng, M.-S., Wang, C.-C., 2014. Investigation of the performance of pulsating heat pipe subject to uniform/alternating tube diameters. *Experimental thermal and fluid science*, 54, pp. 85-92. https://doi.org/10.1016/j.expthermflusci.2014.01.019.

Vakiloroaya, V., Samali, B., Fakhar, A., Pishghadam, K., 2014. A review of different strategies for HVAC energy saving. *Energy conversion and management*, 77, pp. 738-754. https://doi.org/10.1016/j.enconman.2013.10.023.

Wang, J., Ma, H., Zhu, Q., 2015. Effects of the evaporator and condenser length on the performance of pulsating heat pipes. *Applied Thermal Engineering*, 91, pp. 1018-1025. https://doi.org/10.1016/j.applthermaleng.2015.08.106

Wang, Q., Rao, Z., Huo, Y., Wang, S., 2016. Thermal performance of phase change material/oscillating heat pipe-based battery thermal management system. *International Journal of Thermal Sciences*, 102, pp. 9-16. https://doi.org/10.1016/j.ijthermalsci.2015.11.005.

Winkler, M., Rapp, D., Mahlke, A., Zunftmeister, F., Vergez, M., Wischerhoff, E., Clade, J., Bartholomé, K., Schäfer-Welsen, O., 2020. Small-sized pulsating heat pipes/oscillating heat pipes with low thermal resistance and high heat transport capability. *Energies*, 13(7), P. 1736. http://dx.doi.org/10.3390/en13071736.

Xu, R., Li, X., Lei, T., Wu, Q., Wang, R., 2022. Operation characteristics of a gravity pulsating heat pipe under different heat inputs. *International Journal of Heat and Mass Transfer*, 189, P. 122731. https://doi.org/10.1016/j.ijheatmasstransfer.2022.122731.

Yang, H., Wang, J., Wang, N., Yang, F., 2019. Experimental study on a pulsating heat pipe heat exchanger for energy saving in air-conditioning system in summer. *Energy and Buildings*, 197, pp. 1-6. https://doi.org/10.1016/j.enbuild.2019.05.032.

Yang, K.-S., Jiang, M.-Y., Tseng, C.-Y., Wu, S.-K., Shyu, J.-C., 2020. Experimental Investigation on the Thermal Performance of Pulsating Heat Pipe Heat Exchangers. *Energies*, 13(1). https://doi.org/10.3390/en13010269.

Yang, K.-S., Wang, J.-S., Wu, S.-K., Tseng, C.-Y., Shyu, J.-C., 2017. Performance Evaluation of a Desiccant Dehumidifier with a Heat Recovery Unit. *Energies*, 10(12). https://doi.org/10.3390/en101220.06

Youn, Y.J., Kim, S.J., 2012. Fabrication and evaluation of a slicon-based micro pulsating heat spreader. *Sensors and Actuators A: Physical*, 174, pp. 189-197. https://doi.org/10.1016/j.sna.2011.12.006.

Zhan, J., Chen, X., Ji, Y., Zheng, P., Duan, W., 2023 .Experimental study of ethane pulsating heat pipe with varying evaporator lengths based on pulse tube refrigerator. *International Journal of Refrigeration*, 145, pp. 40-49. https://doi.org/10.1016/j.ijrefrig.2022.09.010.

دراسة نظرية وتجريبية لمبادل حراري نابض مملوء بالأسيتون لاستعادة الحرارة المهدرة

نور علي مؤيد *، وائل سامي سرسم

قسم الهندسة الميكانيكية، كلية الهندسة، جامعة بغداد، بغداد، العراق

الخلاصة

في هذا العمل، تم تصميم مبادل حراري لأنبوب حراري نابض رأسي (PHPHE)لاستعادة الحرارة المفقودة، وتبادل الطاقة الحرارية بين تيارين هوائيين في تكوين تدفق معاكس. يتكون المبادل الحراري من ستة صفوف، يتكون كل صف من أنبوب حراري نابض واحد، ولكل PHP ست لفات. كان سائل العمل المستخدم في الأنبوب الحراري هو الأسيتون بنسب ملء 50٪ و60٪ و70٪. تمت دراسة تأثير درجة حرارة مدخل المبخر عند 40 و45 و50 درجة مئوية وسرعة الهواء عند 0.5 و0.7 و0.9 متر/ثانية على أنابيب الحرارة النابضة المكونة من ثلاثة أقسام – المبخر والمكثف والأدياباتي بأبعاد 25 × 25 × 10 سم. في حين تم الحفاظ على درجة حرارة المكثف عند 26 درجة مئوية.م حساب المقاومة الحرارية للنظام وفعاليته وانتقال الحرارة باستخدام برنامج حل المعادلات الهندسية (EES). أظهرت النتائج أن كفاءة الجهاز تتراوح من حوالي 15٪ إلى 32٪. كان أداء الجهاز أفضل عند نسبة تعبئة ٥٠٪ مقارنةً بالنسب الأخرى، محققًا كفاءة عالية عند السرعات المنخفضة.

الكلمات المفتاحية: أنبوب حراري نابض، استعادة الحرارة المهدرة، الأسيتون، المبادل الحراري.